

Electrochemical Quartz Crystal Microgravimetry Study of Metal Deposition from EDTA Complexes

Eimutis Juzeliunas, Howard W. Pickering and Konrad G. Weil

J. Electrochem. Soc. 2000, Volume 147, Issue 3, Pages 1088-1095.
doi: 10.1149/1.1393318

**Email alerting
service**

Receive free email alerts when new articles cite this article - sign up in the box at the top right corner of the article or [click here](#)

To subscribe to *Journal of The Electrochemical Society* go to:
<http://jes.ecsdl.org/subscriptions>

© 2000 ECS - The Electrochemical Society

Electrochemical Quartz Crystal Microgravimetry Study of Metal Deposition from EDTA Complexes

Eimutis Juzeliunas,^{a,z} Howard W. Pickering,* and Konrad G. Weil**

Department of Materials Science and Engineering, The Pennsylvania State University, University Park, Pennsylvania 16802, USA

The electrochemical deposition of metals from Me^{II} (ethylenediaminetetraacetic acid, EDTA) complexes was studied by electrochemical quartz crystal microgravimetry. These investigations are important for the development of environmental clean-up processes, such as remediation of metal-contaminated soils by EDTA and subsequent electrochemical recovery of metal, *in situ* electrokinetic soil remediation, electrochemical gas purification, etc. Deposition of metals frequently encountered in hazardous waste sites, such as Pb, Cu, Cd, Zn, and Ni, was investigated. The potential regions of metal deposition were detected from a distinct increase in electrode mass. We observed reduction of Pb, Cu, Cd, and Zn from both protonated and nonprotonated EDTA complexes. No indications were found for Ni deposition. While diffusion-limited currents of Cu, Cd, and Pb deposition could be achieved, the Zn deposition current was much lower. This can be explained in terms of electrode passivation during Zn deposition. Side reactions were identified, namely, proton reduction, EDTA reduction, and water decomposition.
© 2000 The Electrochemical Society. S0013-4651(98)12-051-7. All rights reserved.

Manuscript submitted December 12, 1998; revised manuscript received November 22, 1999.

Ethylenediaminetetraacetic acid (EDTA), a nontoxic chelating agent, forms very stable complexes with most metal ions (Me) and is widely used in a variety of industrial processes. The chelating properties of EDTA are also very useful in processes of environmental protection. Recently, new electrochemical concepts were suggested for various cleanup applications employing EDTA as complexing agent for different pollutant species. The advantage of electrochemical processes is the employment of electrodes for the supply of electrons instead of chemicals, which usually have to be employed in large amounts in conventional techniques.

Fe^{II}(EDTA) is commonly known as a useful agent for the removal of H₂S,^{1,2} NO,³⁻¹⁰ and NO + SO₂¹¹⁻¹³ from waste gases. NO conversion to nontoxic compounds was achieved by use of dithionite as redox mediator with subsequent electrochemical dithionite regeneration.^{13,14} It has also been shown that direct electrochemical NO conversion on electrodes from Fe^{II}(EDTA)NO is possible.^{15,16}

Numerous investigations were conducted over the last years to study the extraction of toxic metals from polluted soils with chelating agents.¹⁷⁻³¹ Different metals were removed from contaminated soils using EDTA: Cd,¹⁷⁻²⁴ Pb,^{19,20,24-31} Co,^{20,29} Ni,^{20,22,27,29} Cu,^{20,24,27,29,31} Fe,^{20,29} Zn,^{19-22,29,31,32} Mn,^{20,29} As,³¹ Hg,³¹ and Cr.²⁵ Subsequent electrochemical reduction of the Me-EDTA complexes seems to be an effective extension of the remediation process.^{33,34} The conditions need to be found under which metal ions can be electrochemically reduced to the environmentally friendly metallic state and EDTA can be recovered.

A promising alternative in the electrochemical soil cleanup is the *in situ* electrokinetic soil remediation.³⁵⁻³⁷ Electrodes are embedded in the contaminated soil and metals are driven to the electrode by an electric field. Transport of the contaminant occurs by electromigration, electro-osmosis, and electrophoresis.³⁵ However, electrochemical water decomposition can cause a pH increase near the collecting electrodes. Therefore, the solubility of most heavy metals decreases and their mobility is reduced. Introducing EDTA into the reaction zone³⁶ can help to overcome these effects. Hence, the possibility to reduce metal ions from Me(EDTA) complexes at electrodes should be explored.

This overview demonstrates that further development of an electrochemical cleanup process requires basic knowledge regarding the electrochemical behavior of Me^{II}(EDTA) complexes. For electrochemical gas purification one wants to know the potential region

where Me(EDTA) complexes are stable. In contrast, for processes of electrochemical soil remediation the optimal conditions for metal-ion reduction from the Me(EDTA) complexes are of great interest.

It is noteworthy that the study of metal-ion reduction from Me(EDTA) complexes is complicated if conventional dc measurements are used. The electrochemical polarization behavior of Fe^{II}(EDTA) and Fe^{III}(EDTA) was studied over a wide potential range at different pH values in our previous work.^{15,16} Three different electrode reactions proceed simultaneously with the metal deposition, namely, proton reduction, reduction of EDTA, and water decomposition. The partial current of iron deposition is small compared to that of hydrogen evolution. Therefore, voltammetric measurements supply only very limited information about the iron ion reduction. The problem was overcome by the use of electrochemical quartz crystal microgravimetry (EQCM). It could be shown that EQCM gives reliable data for mass changes even in the presence of a rather large hydrogen evolution current.³⁸

In the present study we investigated EDTA complexes of metal ions which are frequently present in hazardous waste sites such as Cu, Cd, Pb, Zn, and Ni. The attention was focused on the determination of the partial current density and the potential region of metal ion deposition from the Me^{II}(EDTA) complexes. Metal deposition was detected by an electrochemical quartz microbalance (EQCM). The balance supplies data on electrode mass changes with high sensitivity and thereby provides for the separation of the partial deposition current from contributions of side reactions.

Experimental

Experiments were conducted using an EQCN-700 electrochemical quartz crystal nanobalance coupled with a PS-205 potentiostat (both Elchema, USA).

Quartz disks, 14 mm diam and 160 μm thick, having a fundamental frequency of $f_0 = 10$ MHz were used. According to Sauerbrey's equation,³⁹ the frequency-to-mass conversion factor is 0.22 Hz cm²/ng when $f_0 = 10$ MHz. The quartz disks were coated with a 10 nm thick chromium underlayer and a 90 nm thick gold overlayer. The geometric area of the working electrode was 0.3 cm². The specimens were used as received from Elchema. Quartz disks were glued to the special window of the electrochemical cell.

The experiments were conducted in 0.5 M Na₂SO₄ supporting electrolyte. The Me(EDTA) complexes were produced by dissolving Na₂EDTA (Fisher Chemical, 100.9%) and metal sulfate (p.a. grade) in the supporting electrolyte at an equimolar ratio. The measurements were taken in solutions deoxygenated with nitrogen gas. The pH corrections were made by using 0.1 N NaOH or 0.1 N H₂SO₄.

* Electrochemical Society Fellow.

** Electrochemical Society Active Member.

^a Permanent address: Institute of Chemistry, 2600 Vilnius, Lithuania.

^z E-mail: ejuzel@klt.mii.lt

An Ag/AgCl reference electrode was used; the counter electrode was a platinum wire. The Rotacell electrochemical cell system RTC-100 and the Faraday cage 702 (both designed by Elchema, USA) were used.

Results and Discussion

Na₂SO₄ and EDTA solutions.—Prior to the study of the Me(EDTA) complexes one has to elucidate the EQCM behavior in the blank supporting solution as well as in the metal-free EDTA solution. Figure 1 shows a cyclic voltammogram and the simultaneous mass change for a gold electrode in the supporting electrolyte adjusted to pH 3 (this value is typical for the Me(EDTA) solutions studied). While no remarkable faradaic process is observed during the potential sweep from $E = 0.0$ V to $E \approx -0.4$ V, an increase in electrode mass is observed in this region. A similar phenomenon was also reported for platinum electrodes in acid media.^{38,40,41} One may assume that hydrogen atoms are adsorbed on the electrode during the negative potential sweep and water molecules are bonded with the surface via these hydrogen atoms.^{40,41} As a consequence, the surface becomes more hydrophilic, *i.e.*, develops a thicker adhering solution layer. This explanation is supported by infrared spectroscopy, which shows that hydrogen atoms are adsorbed at potentials below 0 V $V_{\text{Ag/AgCl}}$ in acid solutions.^{42,43}

At potentials below $E \approx -0.4$ V a cathodic current with a peak at $E \approx -0.8$ V appears. This current is not observed in neutral supporting solution and therefore may be ascribed to proton reduction. The mass gain stops when the proton reduction starts. The slight decrease in mass below *ca.* -0.5 V may be due to replacement of liquid by gas bubbles during hydrogen evolution on the electrode.

Two mass-gain zones are observed above *ca.* 0.3 V in Fig. 1. There is no remarkable faradaic process in the first mass-gain zone (*ca.* 0.3-0.8 V), which is the so-called double-layer region. A similar phenomenon can be observed in HClO₄ and HNO₃ solutions.⁴⁴⁻⁴⁶

Bruckenstein and Shay⁴⁴ relate this mass increase to anion adsorption. Gordon and Johnson,⁴⁵ however, attribute this mass increase to increased surface hydration as a consequence of the formation of Au(OH)_{*a*} ($a \ll 1$). The second mass-gain region in Fig. 1 and the corresponding limiting current (above *ca.* 0.8 V) are due to the gold oxide formation on the surface.^{44,45} Recently, this conclusion was confirmed also by simultaneous measurements by EQCM and optical reflectivity.⁴⁶ The sharp cathodic peak, which appears at *ca.* 0.7 V during the reverse potential sweep, is due to the reduction of the oxide layer developed during the positive potential sweep.

Figure 2 shows a voltammogram and the corresponding mass-change curve obtained from a solution containing Na₂EDTA. Anodic EDTA decomposition is observed above *ca.* 0.5 V. Numerous products of the anodic EDTA decomposition in Na₂SO₄ + H₂SO₄ solution (pH 0.35-4.0) were identified by Johnson *et al.*,⁴⁷ *e.g.*, CO₂, formaldehyde, iminodiacetic acid, ethylenedinitrioltriacetic acid, ethylenediglycine, glycine, 2-oxo-1-piperazineacetic acid, aminoethylglycine, 2-oxopiperazine, and ethylenediamine. Thus, the reaction pathways seem to be rather complicated.

Two distinct cathodic currents are observed during the negative potential sweep in acid EDTA solution (A and B in Fig. 2). Peak A appears at the same potential as in the EDTA-free solution (Fig. 1). Furthermore, peak A is absent in solutions with pH values of 4.6 and 6.9 (Fig. 3). These data imply that current A is due to H₃O⁺ reduction. Current B should be attributed to the cathodic decomposition of EDTA, which was discussed in detail.¹⁶ The distinct current in pH 4.6 solution indicates easy EDTA decomposition, whereas the process is retarded in neutral media (pH 6.9, Fig. 3). These data confirm the well-known fact that the protonated forms of weak organic acids can be reduced more easily than the deprotonated forms.⁴⁸

The mass-change curve in the solution containing EDTA (Fig. 2) is similar to that in the blank supporting electrolyte (Fig. 1). Thus,

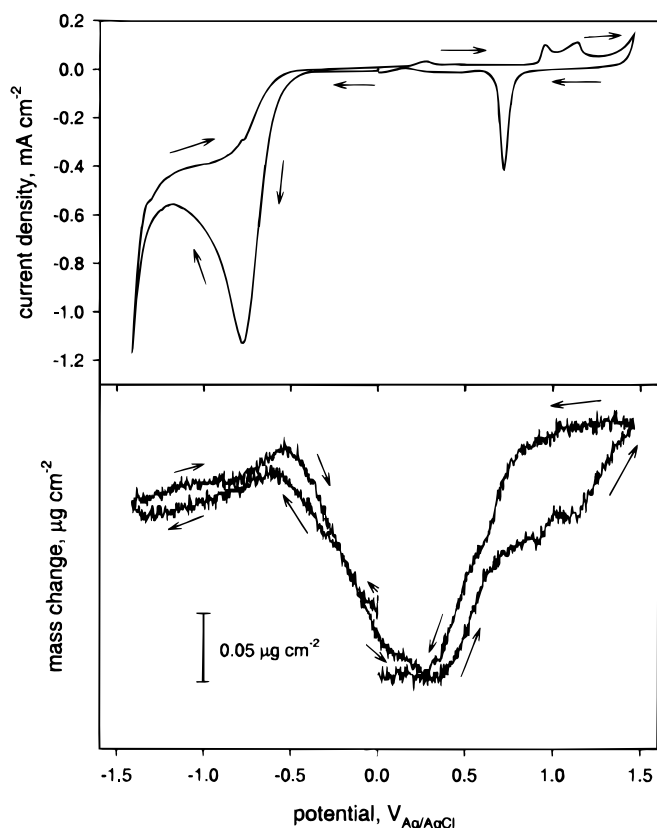


Figure 1. EQCM data and cyclic voltammogram recorded simultaneously in 0.5 M Na₂SO₄ solution adjusted to pH 3. Cathodic potential sweep 20 mV s⁻¹ was started at 0.0 V.

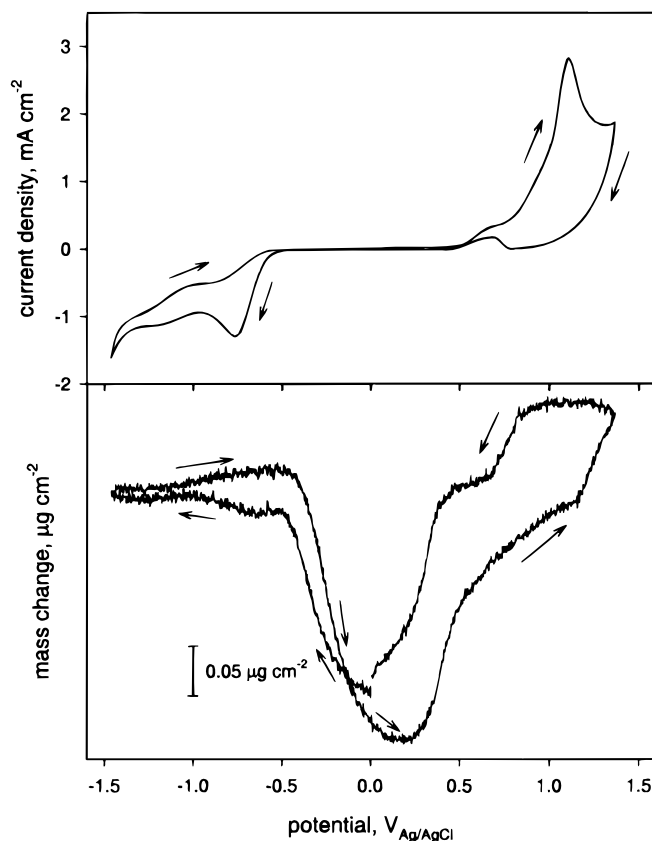


Figure 2. EQCM data and cyclic voltammogram recorded simultaneously in 0.5 M Na₂SO₄ + 10 mM Na₂EDTA solution adjusted to pH 3. Cathodic potential sweep 20 mV s⁻¹ was started at 0.0 V.

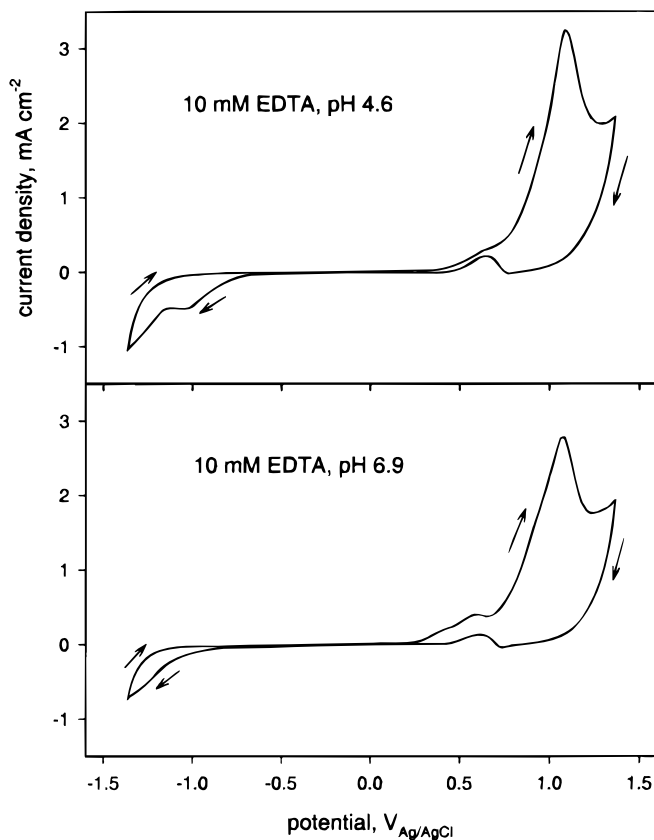
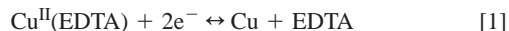


Figure 3. Cyclic voltammograms recorded in 0.5 M Na₂SO₄ + 10 mM Na₂EDTA solution adjusted to pH 4.6 (upper) and pH 6.9 (lower). Cathodic potential sweep 20 mV s⁻¹ was started at 0.0 V.

the mass vs. potential change in the EDTA solution may be explained in the same way as was done for the supporting electrolyte. In the region $E > 1.0$ V EDTA oxidation is accompanied by oxide-layer formation. It may be assumed that the oxide film has an inhibiting effect on the EDTA oxidation, which leads to the hysteresis in the reverse potential sweep. An analogous conclusion was drawn studying EDTA oxidation on Pt electrodes.¹⁶

Cu^{II}(EDTA) solutions.—Figure 4 shows the polarization behavior and the mass-change curve for a solution containing 10 mM Cu^{II}(EDTA) at pH 2.9. When the potential is swept from $E = 0.0$ V in negative direction, a cathodic current, i_1 , appears below ca. -0.4 V. A simultaneous increase in the electrode mass is observed, which indicates copper deposition



The deposition rate reaches a limiting value below -0.6 V. This can be seen from the appearance of a limiting current $i = -0.4$ mA cm⁻² and a constant mass gain $dm/dt = 0.11$ μg s⁻¹. According to Faraday's law, this mass gain rate corresponds to a current $i = -0.33$ mA cm⁻², which is in satisfactory agreement with the observed value.

From earlier voltammetric measurements a limiting diffusion current for iron deposition from 5 mM Fe^{II}(EDTA) solution was found to be $i = 0.17$ mA cm⁻², while EQCM data lead to $i = 0.2$ mA cm⁻².³⁸ These rates are about half those measured for copper reduction from 10 mM Cu^{II}(EDTA) solutions. This indicates that both ions are reduced under diffusion control and that the diffusivities of Cu^{II}(EDTA) and Fe^{II}(EDTA) do not differ very much.

A further current increase is observed in Fig. 4 below ca. -0.75 V, which does not affect the mass gain rate. In order to make current contributions more visible, a higher potential sweep rate was applied (Fig. 5). Indeed, two current peaks A and B appear in Fig. 5 after the

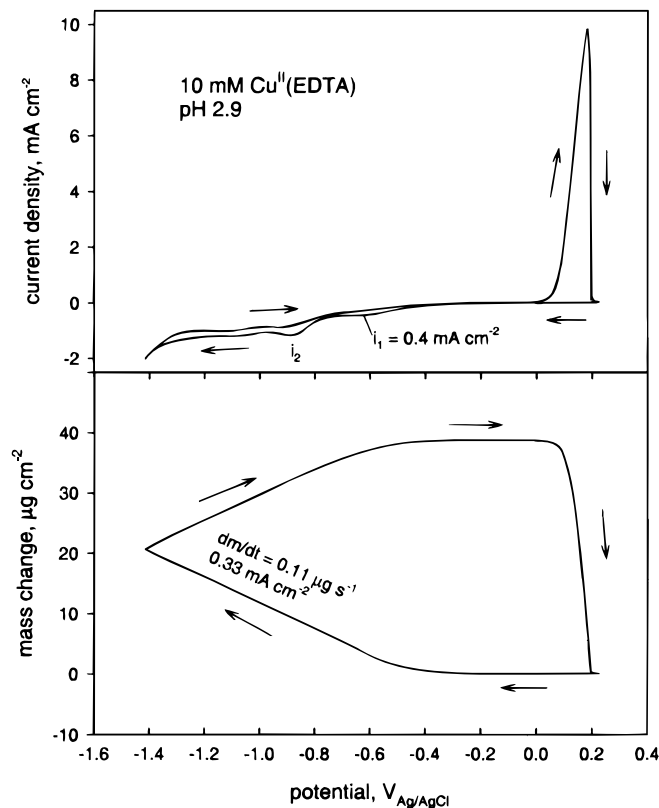


Figure 4. EQCM data and cyclic voltammogram recorded simultaneously in 0.5 M Na₂SO₄ + 10 mM Cu^{II}(EDTA) solution (pH 2.9). Cathodic potential sweep 5 mV s⁻¹ was started at 0.0 V.

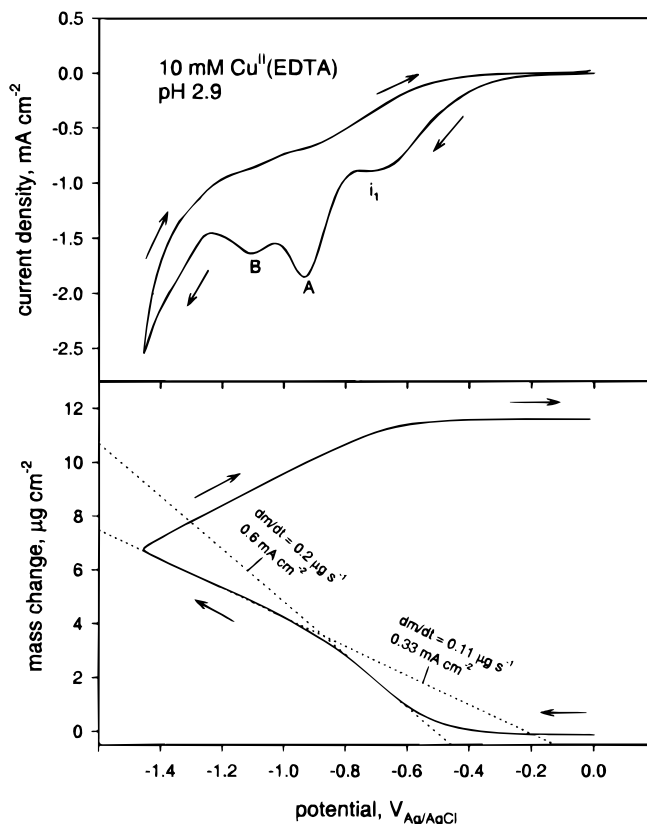


Figure 5. EQCM data and voltammetric characteristic recorded simultaneously in 0.5 M Na₂SO₄ + 10 mM Cu^{II}(EDTA) of pH 2.9. Potential sweep rate 20 mV s⁻¹.

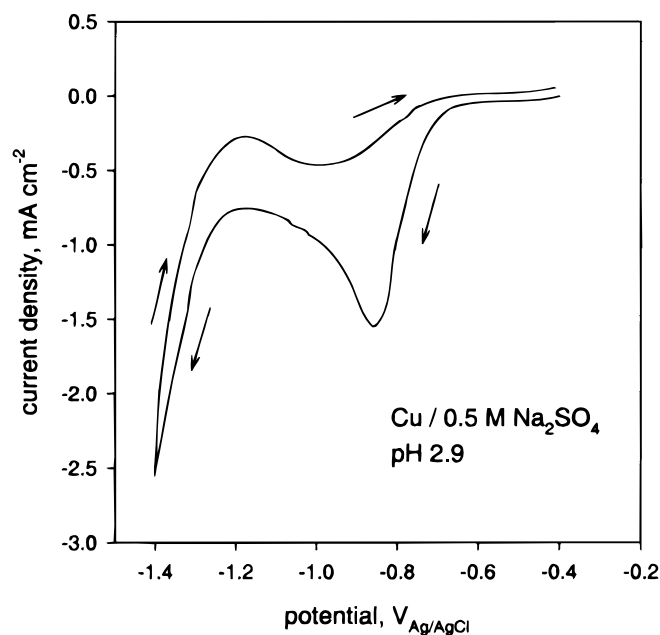


Figure 6. Voltammogram of a copper electrode in 0.5 M Na₂SO₄ adjusted to pH 2.9. Potential sweep rate 20 mV s⁻¹. The gold electrode was preplated with copper from a 0.5 M Na₂SO₄ + 10 mM Cu^{II}(EDTA) of pH 2.9 at $E = -0.7$ V for 4 min. Then the solution was replaced by the deaerated solution under investigation.

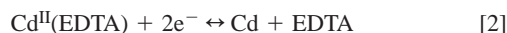
copper deposition current (i_1). i_1 is higher in the first deposition stage. This may reflect the development of the diffusion layer during the polarization. It should be mentioned that a limiting current and a steady-state diffusion profile can only be observed at low scan rates, at a scan rate of 20 mV/s the voltammogram indicates a $t^{1/2}$ behavior, in contrast to what is seen in Fig. 4 at a scan rate of 5 mV/s.

The current A can be attributed to H₃O⁺ reduction on deposited copper. A similar current peak can be seen in Fig. 6 on a copper electrode in EDTA-free solution. Consequently, current B can be attributed to EDTA reduction, as was already reported by Müller *et al.*⁴⁹ They found the following reduction products from Cu^{II}(EDTA): formaldehyde, formiate, glycoacid, acetate, ammonium, monomethylamine, and ethylenediamine.

Figure 7 depicts results obtained in Cu^{II}(EDTA) solution at pH 7. Copper deposition starts below *ca.* -0.7 V, as indicated by an increase in electrode mass and a corresponding cathodic current. Thus, copper deposition in neutral solution occurs at more negative potentials as compared to acid solutions (Fig. 4 and 5). However, the diffusion-limited reduction rate, derived from the steady-state slope dm/dt (Fig. 7), is of the same magnitude as in more acid solutions (Fig. 4).

The anodic copper dissolution takes place above *ca.* 0.0 V in both acid and neutral solutions, as can be seen from Fig. 4 and 7. The dissolution is complete since the electrode mass returns to its initial value at $E = 0.0$ V.

Cd^{II}(EDTA) solutions.—Figures 8 and 9 show simultaneous EQCM and voltammetric curves in acid and almost neutral Cd^{II}(EDTA) solutions, respectively. The cadmium deposition reaction



is indicated in the acid solution below *ca.* -0.6 V by the distinctive increase in the electrode mass. The current peak at $E \approx -0.8$ V is typical for proton reduction (Fig. 1 and 2). The partial current of Reaction 2 is very low compared to the peak current. So, the mass gain rate at $E \approx -0.8$ V yields a partial ion reduction current $i = -0.072$ mA cm⁻², whereas the total current is much higher. The small peak at $E \approx -1.1$ V should be attributed to EDTA reduction, as it follows from current B in Fig. 2, established in a metal-free EDTA solution.

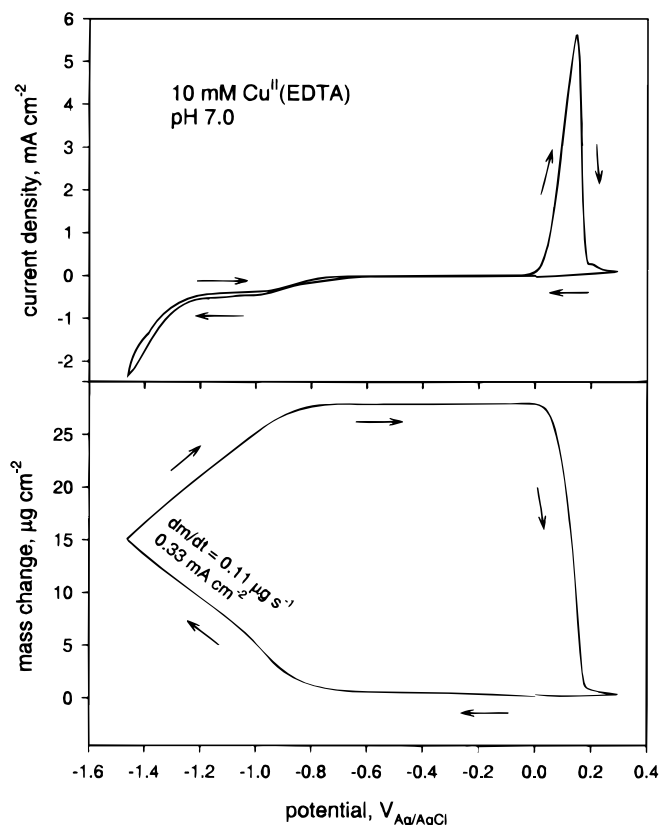


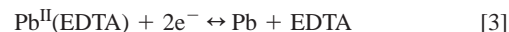
Figure 7. EQCM data and cyclic voltammogram recorded simultaneously in 0.5 M Na₂SO₄ + 10 mM Cu^{II}(EDTA) solution (pH 7.0). Cathodic potential sweep 20 mV s⁻¹ was started at 0.0 V.

Cadmium deposition in the pH 6.6 solution starts at $E \approx -1.0$ V (Fig. 9), *i.e.* at more negative potentials than in the pH 3.28 solution (*ca.* -0.6 V, Fig. 8). Consequently, the process is more favored in acid medium.

The EQCM curves yield the limiting deposition current $i = -0.23$ mA cm⁻² in acid solution (Fig. 8) and $i = -0.19$ mA cm⁻² in the neutral one (Fig. 9). These values are very close to the values established for iron and copper deposition which were concluded to be diffusion limited currents. Therefore, it may be supposed that electrochemical deposition of cadmium from Cd^{II}(EDTA) solutions, takes place as a diffusion-limited process as well.

During the reverse potential sweep, anodic cadmium dissolution starts actually at the same potentials at which the deposition started, *i.e.*, at $E \approx -0.6$ V in the acid solution (Fig. 8) and $E \approx -1.0$ V in the neutral one (Fig. 9). The mass decrease vanishes at about 0.0 V, and the mass remains constant over a wide potential region (until $E \approx 1.2$ V). Hence, some cadmium is still present on the electrode in form of scarcely soluble compounds. A further stripping process takes place above 1.2 V, *i.e.*, in the region where anodic EDTA and water decomposition takes place. During a subsequent reverse potential sweep, a cathodic peak at $E \approx 0.7$ V and the simultaneous mass decrease indicate the reduction of a gold oxide layer, as discussed previously (Fig. 1). Even after the complete cycle at $E = 0.0$ V, a residual mass gain is observed indicating strong bonding between the nonsoluble compound and the electrode surface (Fig. 8).

Pb^{II}(EDTA) solutions.—According to Fig. 10, lead deposition from a solution of pH 3.12



takes place below *ca.* -0.7 V (Fig. 10). The current peak at $E \approx -0.8$ V is due to proton reduction, as discussed earlier. The slope dm/dt around $E = -0.9$ V leads to a current density of Reaction 3 of $i = -0.29$ mA cm⁻². The total current at this potential is $i =$

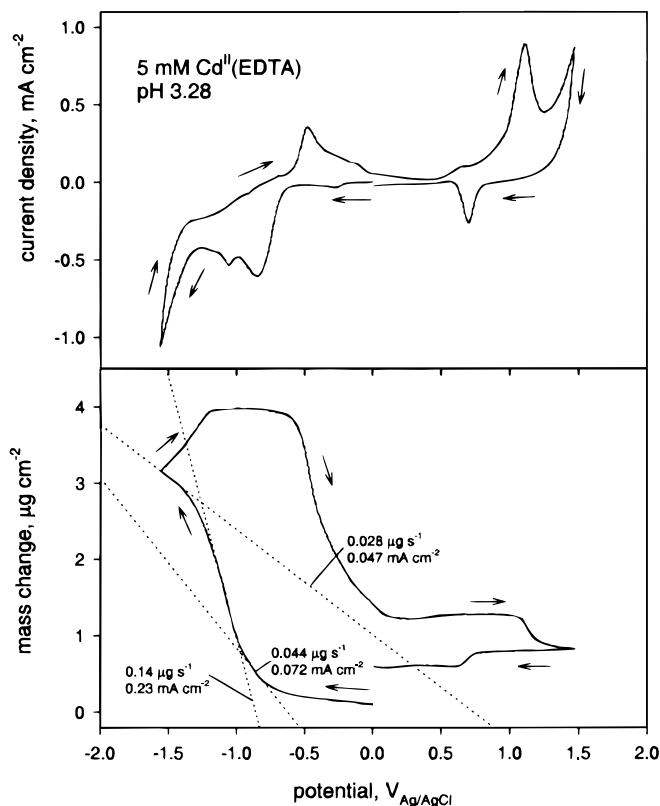


Figure 8. EQCM data and cyclic voltammogram recorded simultaneously in 0.5 M Na₂SO₄ + 5 mM Cd^{II}(EDTA) solution (pH 3.28), potential sweep rate 20 mV s⁻¹.

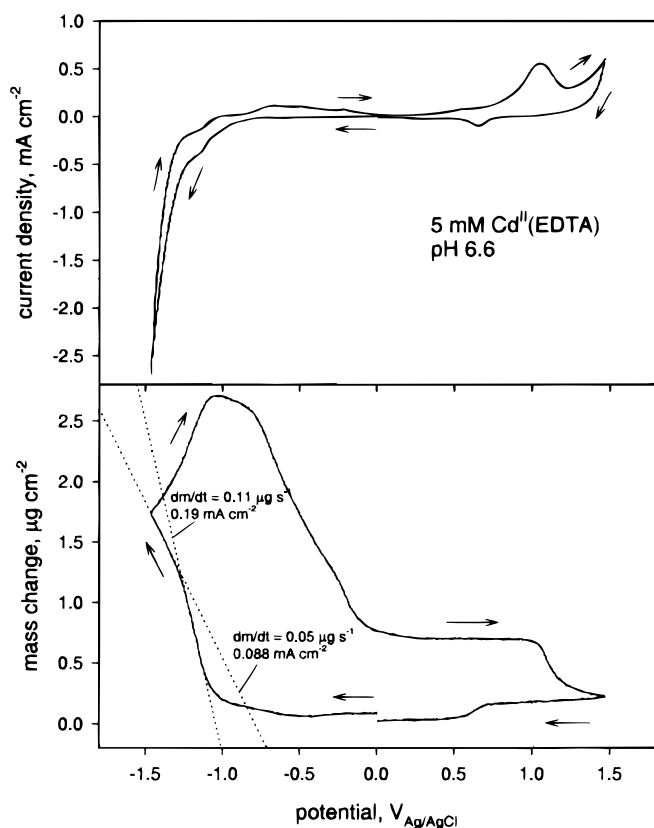


Figure 9. EQCM data and cyclic voltammogram recorded simultaneously in 0.5 M Na₂SO₄ + 5 mM Cd^{II}(EDTA) solution (pH 6.6), potential sweep rate 20 mV s⁻¹.

-0.45 mA cm⁻². The difference of these currents equals the rate of proton reduction. At $E > -1.2$ V, a further current contribution appears in Fig. 10 which can be assigned to EDTA reduction. The limiting deposition current in Fig. 10 is $i = -0.17$ mA cm⁻², which corresponds well to the diffusion-limited currents discussed previously.

One can see from Fig. 10 that anodic lead oxidation starts at about -0.6 V, indicated by the anodic current A and the simultaneous decrease in mass. Lead ions produced by the anodic current may be stabilized by reaction with EDTA, which is present in the vicinity of the electrode after the cathodic Reaction 3. Two sharp current peaks B and C are accompanied by distinct increases in electrode mass. Obviously, scarcely soluble compounds are formed on the electrode surface associated with these currents. Current B can be attributed to the reaction



The equilibrium potential for this reaction can be calculated from⁵⁰

$$E = -0.113 - 0.0295 \text{ pH} - 0.0148 \log a_{\text{SO}_4^{2-}} \quad [5]$$

Under the conditions of Fig. 10 one obtains $E = -0.426$ V_{Ag/AgCl}, compared to $E \approx -0.44$ V for the onset of current B. Current C may be ascribed to the reaction



Its equilibrium potential is⁵⁰

$$E = 0.03 - 0.044 \text{ pH} - 0.0074 \log a_{\text{SO}_4^{2-}} = -0.330 \text{ V}_{\text{Ag/AgCl}} \quad [7]$$

under the conditions of Fig. 10. The onset potential of current C is $E = -0.35$ V

Figure 11 shows EQCM and voltammetric data obtained in Pb^{II}(EDTA) solution at pH 6.34. According to the mass curve, lead deposition starts below *ca.* -1.1 V. Comparing this potential with

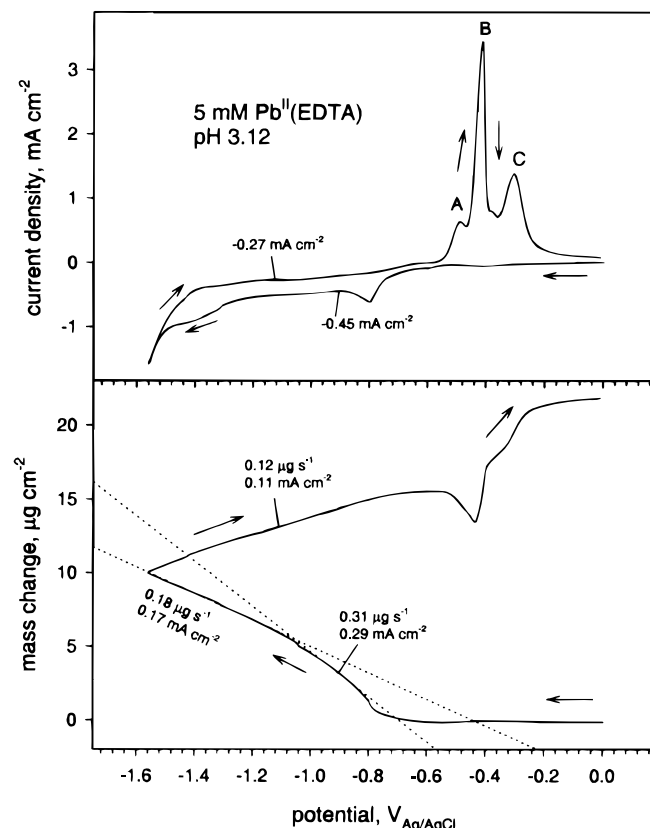


Figure 10. EQCM data and voltammetric characteristic recorded simultaneously in 0.5 M Na₂SO₄ + 5 mM Pb^{II}(EDTA) solution (pH 3.12), potential sweep rate 20 mV s⁻¹.

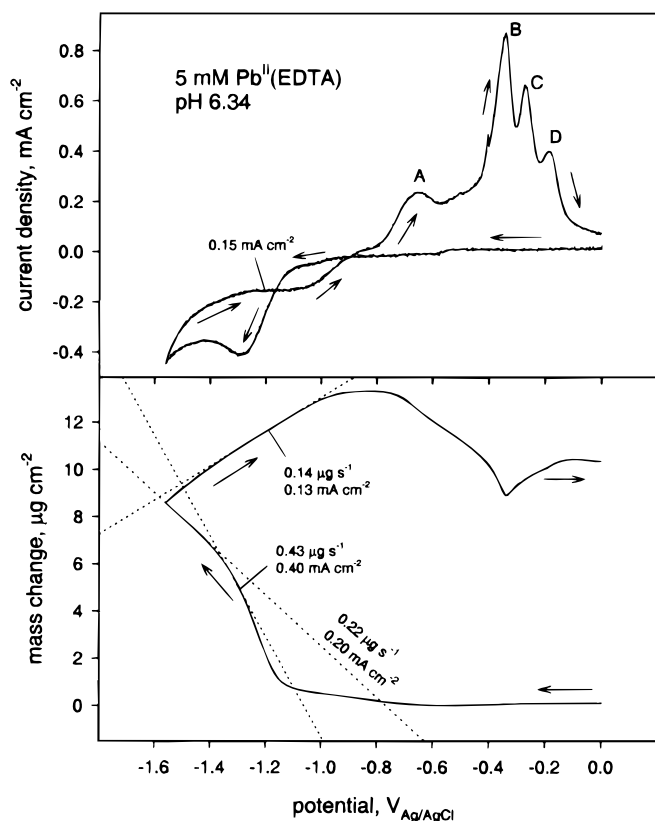
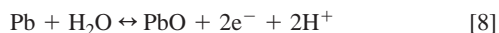


Figure 11. EQCM data and voltammetric characteristic recorded simultaneously in 0.5 M Na₂SO₄ + 5 mM Pb^{II}(EDTA) solution (pH 6.34), potential sweep rate 20 mV s⁻¹.

the analogous one in Fig. 10, we can conclude that lead deposition is more favored in acid media. The current maximum $i \approx -0.4$ mA cm⁻² at $E \approx -1.3$ V coincides well with the current derived from the dm/dt slope. Upon sweeping the potential in positive direction, a limiting current $i = -0.15$ mA cm⁻² also coincides well with the value $i = 0.13$ mA cm⁻² calculated from dm/dt slope. Thus, there were no side reactions found along with lead deposition prior to the beginning of water decomposition.

The anodic lead dissolution in almost neutral solution (Fig. 11) starts at about -0.85 V. The anodic current A and the simultaneous decrease in mass suggest the anodic reversal of Reaction 3. A subsequent mass gain above *ca.* -0.34 V occurs when the current decreases after peak B. This behavior may be explained by lead oxide formation



the potential of which is⁵⁰

$$E = -0.356 - 0.0295 \log a_{\text{SO}_4^{2-}} = -0.349 \text{ V} \quad [9]$$

The nature of currents C and D needs to be identified in further investigations.

The EQCM data in both acid and neutral solutions indicate that in order to dissolve the deposited lead the formation of hardly soluble species must be avoided.

Zn^{II}(EDTA) solutions.—Results obtained in acid Zn^{II}(EDTA) solution of pH 3.0 are shown in Fig. 12. A zinc deposition reaction starts below *ca.* -0.7 V. A constant mass gain rate $dm/dt = 0.038$ μg s⁻¹ is observed in the region between -1.1 and -1.5 V, which corresponds to an ion reduction current $i = 0.11$ mA cm⁻². This current is somewhat lower than ion reduction currents observed in acid solutions of other metals: copper $i = 0.17$ mA cm⁻² [Fig. 4, when corrected to

5 mM Cu^{II}(EDTA)], cadmium $i = 0.23$ mA cm⁻² (Fig. 8), lead $i = 0.17$ mA cm⁻² (Fig. 10), iron $i = 0.2$ mA cm⁻².³⁸ The deposition reaction is inhibited in the region of water decomposition. Indeed, no mass change is observed between -1.6 and -1.4 V in the reverse potential sweep. Zinc dissolution only occurs above *ca.* -1.1 V, as can be seen from the pronounced mass decrease and the corresponding anodic current. Zinc stripping is completed at $E \approx -0.4$ V.

The data in Fig. 12 show that the partial current of zinc deposition is only a small fraction of the total current. Therefore, the dominant cathodic process is H₃O⁺ reduction. This is a good example to demonstrate the usefulness of the EQCM in cases where an ion deposition current is masked by a much higher hydrogen evolution current.

Figure 13 gives data obtained for a Zn^{II}(EDTA) solution of pH 7.2, *i.e.*, when H₃O⁺ ion concentration is negligible. Zinc deposition in this solution takes place below -0.8 V, as is evident from the mass increase and the corresponding cathodic current. The current peak at *ca.* -1.05 V is most likely due to the reduction of EDTA (Fig. 2), which is present in the vicinity of the electrode after the cathodic Zn^{II}(EDTA) deposition. The dissolution reaction starts at $E \approx -1.0$ V. The accumulation of scarcely soluble compounds on the surface is evident above -0.75 V.

The steady-state mass gain in Fig. 13, $dm/dt = 0.02$ μg s⁻¹, corresponds to a current density $i = 0.06$ mA cm⁻². The limiting current obtained from the voltammogram is $i = 0.08$ mA cm⁻². Much higher currents were determined in neutral solutions for other metals: $i = 0.17$ mA cm⁻² for copper [Fig. 7, when corrected to 5 mM Cu^{II}(EDTA)], $i = 0.19$ mA cm⁻² for cadmium (Fig. 9), and $i = 0.2$ mA cm⁻² for lead (Fig. 11). This difference implies that under the conditions studied the zinc electrode is quite passive. A possible reason for this is considered.

A gold electrode was immersed in 5 mM Zn^{II}(EDTA) of pH 7.4 and polarized to $E = -0.7$ V by a potential step (Fig. 14). The steady-state cathodic current is negligible at this potential. While a

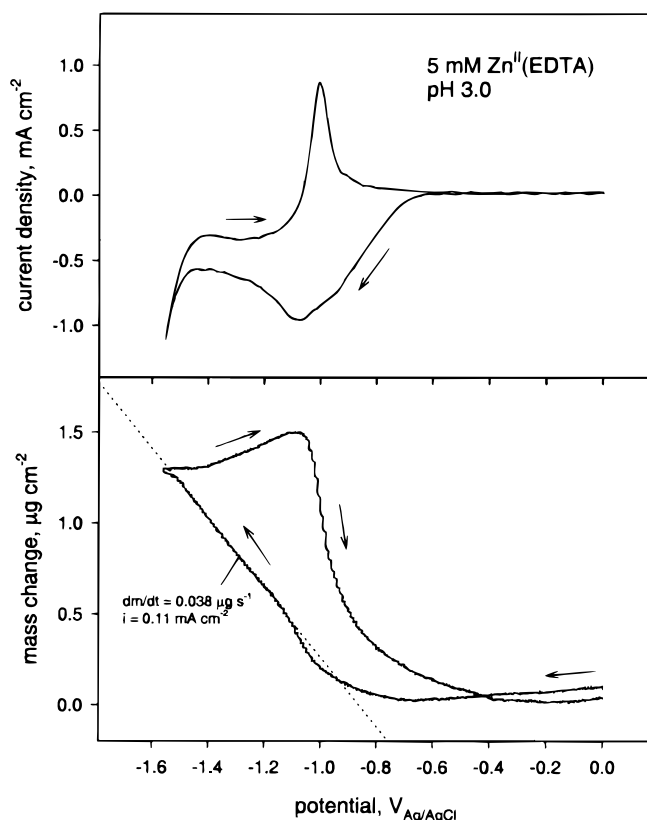


Figure 12. EQCM data and cyclic voltammogram recorded simultaneously in 0.5 M Na₂SO₄ + 5 mM Zn^{II}(EDTA) solution (pH 3.0), potential sweep rate 20 mV s⁻¹.

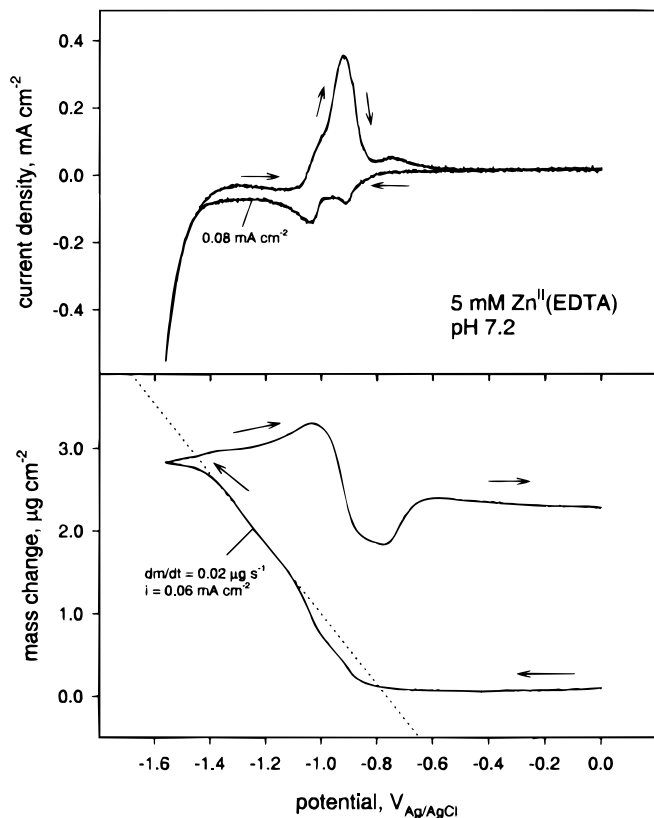


Figure 13. EQCM data and cyclic voltammogram recorded simultaneously in 0.5 M Na_2SO_4 + 5 mM $\text{Zn}^{\text{II}}(\text{EDTA})$ solution (pH 7.2), potential sweep rate 5 mV s^{-1} .

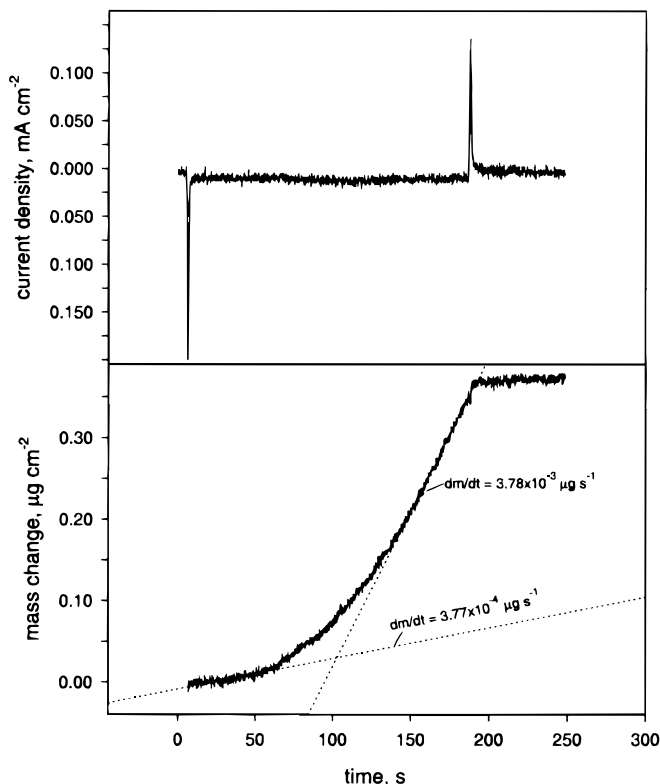


Figure 14. Current and electrode mass vs. time for a gold electrode after a potential step from $0.18 \text{ V}_{\text{Ag}/\text{AgCl}}$ to $-0.7 \text{ V}_{\text{Ag}/\text{AgCl}}$ in 0.5 M Na_2SO_4 + 5 mM $\text{Zn}^{\text{II}}(\text{EDTA})$ solution (pH 7.4).

faradaic process is absent, an electrode mass gain can be seen from Fig. 14. This mass gain occurs very slowly at the beginning ($dm/dt = 3.77 \times 10^{-4} \mu\text{g s}^{-1}$), however, with time it reaches an approximately ten times higher value. The total mass gain is $\Delta m \approx 0.38 \mu\text{g cm}^{-2}$, which remains for a long time unchanged when the potential is returned to the open-circuit value. (Let us remember that the mass of a monolayer of a metal in the underpotential region is $0.16 \mu\text{g cm}^{-2}$ for Cd and $0.14 \mu\text{g cm}^{-2}$ for Cu.⁵¹) Hence, the mass gain is caused by a few monolayers only. It is likely that a scarcely soluble compound precipitates onto the surface, which gives rise to the passivity of the electrode in the region of zinc deposition. Presumably, $\text{Zn}(\text{OH})_2$ could precipitate on the electrode.

It follows from the stability constant $\log K = 16.5$ ⁵² that about $5.6 \times 10^{-9} \text{ mol/L}$ of noncomplexed Zn(II) ions are present in a solution containing 5 mM $\text{Zn}^{\text{II}}(\text{EDTA})$. At negative potentials, Zn(II) ions can adsorb on the Au surface and $\text{Zn}^{\text{II}}(\text{EDTA})$ can act as a Zn(II) ion donor. In spite of the very low concentration, the transfer rate of Zn(II) to the electrode could be high enough due to a very thin diffusion layer caused by a relatively high donor concentration. With time, the surface concentration of Zn(II) increases sufficiently to cause precipitation of $\text{Zn}(\text{OH})_2$. Certainly, this proposition needs further verification by experiments.

Ni^{II}(EDTA) solutions.—There is no indication from either current measurement or from mass determination that Ni deposition occurs from acid $\text{Ni}^{\text{II}}(\text{EDTA})$ solution (Fig. 15). The mass change curve in this case is similar to that in metal-free EDTA solution (Fig. 2). The mass increase between 0.0 and -0.8 V is due to proton adsorption and the increase in surface hydrophilicity as discussed previously. There is no distinctive mass increase indicating metal deposition below *ca.* -0.8 V . The electrode was polarized down to $E = -1.8 \text{ V}$ and the gold film on the quartz was destroyed by hydrogen gas; however, no indications of Ni deposition were detected.

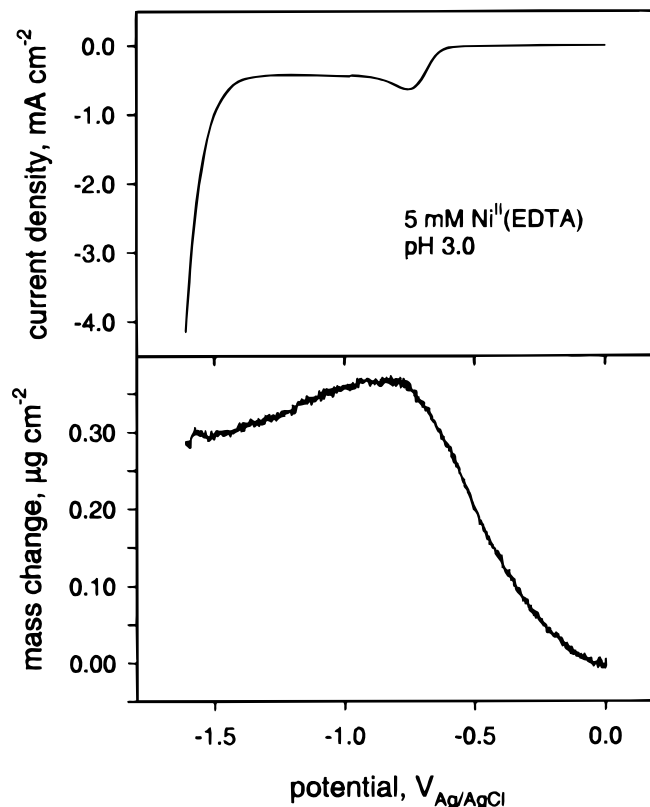


Figure 15. EQCM data and voltammogram recorded simultaneously in 0.5 M Na_2SO_4 + 5 mM $\text{Ni}^{\text{II}}(\text{EDTA})$ solution (pH 3), potential sweep rate 5 mV s^{-1} .

Therefore, future efforts should be focused on searching for a catalyst, which facilitates Ni reduction.

Conclusions

The electrochemical deposition of Cu, Pb, Cd, Zn, and Ni from $\text{Me}^{\text{II}}(\text{EDTA})$ complexes was studied by EQCM in acid (*ca.* pH 3) and neutral (*ca.* pH 7) solutions. These investigations are important for environmental clean-up processes, such as remediation of soil by EDTA and subsequent electrochemical recovery of metal, electrokinetic soil remediation, electrochemical gas purification, etc. It was detected from the distinct increase in electrode mass that Cu, Cd, Pb, and Zn can be reduced from their respective EDTA complexes, whereas no indications were found for Ni reduction. In contradiction to Allen and Chen,³³ we observed reduction of the metals from both protonated and nonprotonated EDTA complexes. The reduction was more favored in acid solutions.

Copper deposition, indicated by a distinct increase of the electrode mass, occurs below $-0.4 V_{\text{Ag}/\text{AgCl}}$ from acid solution and below $-0.7 V_{\text{Ag}/\text{AgCl}}$ from a neutral one. Three side reactions, namely, proton reduction, EDTA reduction, and water decomposition were identified in distinct potential regions below the copper deposition region. The EQCM data during the reverse potential sweep indicated complete copper dissolution above $0.0 V_{\text{Ag}/\text{AgCl}}$.

The cadmium deposition reaction was indicated below $-0.6 V_{\text{Ag}/\text{AgCl}}$ in acid solution and below $-1.0 V_{\text{Ag}/\text{AgCl}}$ in the neutral one. The partial current of cadmium deposition in acid solution is very low compared to the total current, indicating the deposition reaction to be accompanied by proton reduction. Cadmium anodic stripping may be complicated due to formation of scarcely soluble species on the electrode surface.

Lead deposition from acid $\text{Pb}^{\text{II}}(\text{EDTA})$ solutions can be observed below 0.7 V, simultaneously with proton reduction. In neutral solution, lead deposition takes place below -1.1 V. In neutral solution the experimental lead deposition current agrees well with that calculated from the slope dm/dt . Hence, there is no side reaction in the region prior to water decomposition.

Anodic lead oxidation occurs above -0.6 V in an acid solution and above -0.85 V in a neutral one. During the reverse potential sweep we see the formation of scarcely soluble compounds on the electrode. From the potentials at which the deposition reactions start, one can identify $\text{PbO} \cdot \text{PbSO}_4$ and $3\text{PbO} \cdot \text{PbSO}_4 \cdot \text{H}_2\text{O}$, respectively, as the deposited products.

Zinc deposition occurs from acid solution below -0.7 V and is accompanied by proton reduction. Deposition in neutral solution was observed actually in the same region. The limiting currents of zinc deposition from neutral solution are much lower than the analogous currents determined for other metals. This difference may be due to the precipitation of $\text{Zn}(\text{OH})_2$ onto the electrode prior to zinc deposition.

The limiting currents derived from the dm/dt slopes for Cu, Cd, and Pb deposition were close to the diffusion-limited current for iron ion reduction from $\text{Fe}^{\text{II}}(\text{EDTA})$. This implies that the deposition of these metals also proceeds under diffusion control

Acknowledgments

This work was supported by the National Science Foundation, grant no. 9612303. E.J. thanks the American Chemical Society for a stipend.

References

1. J. F. Demmink, H. J. Wubs, and A. A. C. M. Beenackers, *Ind. Eng. Chem. Res.*, **33**, 2989 (1994).
2. H. J. Wubs and A. A. C. M. Beenackers, *AIChE J.*, **40**, 433 (1994).
3. M. Teramoto, S. Hiramine, Y. Shimada, Y. Sugimoto, and H. Teranishi, *J. Chem. Eng. Jpn.*, **11**, 450 (1978).
4. D. Littlejohn and S. G. Chang, *J. Phys. Chem.*, **86**, 537 (1982).
5. S. G. Chang, D. Littlejohn, and S. Lynn, *Environ. Sci. Technol.*, **17**, 649 (1983).
6. W. Weisweiler, R. Blumhofer, and T. Westermann, *Chem. Eng. Process.*, **20**, 155 (1986).
7. S. A. Bedell, S. S. Tsai, and R. R. Grinstead, *Ind. Eng. Chem. Res.*, **27**, 2092 (1988).
8. L. Huasheng and F. Wenchi, *Ind. Eng. Chem. Res.*, **27**, 770 (1988).
9. S. S. Tsai, S. A. Bedell, L. H. Kirby, and D. J. Zabcik, *Environ. Prog.*, **8**, 126 (1989).
10. J. F. Demmink, I. C. F. van Gils, and A. A. C. M. Beenackers, *Ind. Eng. Chem. Res.*, **36**, 4914 (1997).
11. E. Sada, H. Kumazawa, Y. Sawada, and T. Kondo, *Ind. Eng. Chem. Process Des. Dev.*, **21**, 771 (1982).
12. S.-M. Yih and Ch.-W. Lii, *Chem. Eng. J.*, **42**, 145 (1989).
13. K. Jüttner, G. Kreysa, K.-H. Kleifges, and R. Rottmann, *Chem.-Ing.-Tech.*, **66**, 82 (1994).
14. K. H. Kleifges, G. Kreysa, and K. Jüttner, *J. Appl. Electrochem.*, **27**, 1012 (1997).
15. K.-H. Kleifges, E. Juzeliunas, and K. Jüttner, *Electrochim. Acta*, **42**, 2947 (1997).
16. E. Juzeliunas and K. Jüttner, *J. Electrochem. Soc.*, **145**, 53 (1998).
17. M. J. McLaughlin, N. A. Maier, G. E. Rayment, L. A. Sparrow, G. Berg, A. McKay, P. Milham, R. H. Merry, and M. K. Smart, *J. Environ. Qual.*, **26**, 1644 (1997).
18. A. Franchi and A. P. Davis, *Water, Air, Soil Pollut.*, **100**, 181 (1997).
19. Zh. Li and L. M. Shuman, *Environ. Pollut.*, **95**, 219 (1997).
20. B. E. Davies, *Water, Air, Soil Pollut.*, **94**, 85 (1997).
21. T. Streck and J. Richter, *J. Environ. Qual.*, **26**, 49 (1997).
22. Z. Li and L. M. Shuman, *Sci. Total Environ.*, **191**, 95 (1996).
23. J. Hong and P. Pintauro, *Water, Air, Soil Pollut.*, **86**, 35 (1996).
24. J. Hong and P. Pintauro, *Water, Air, Soil Pollut.*, **87**, 73 (1996).
25. J. Pichtel and T. M. Pichtel, *Environ. Eng. Sci.*, **14**, 97 (1997).
26. L. Q. Ma, A. L. Choate, and G. N. Rao, *J. Environ. Qual.*, **26**, 801 (1997).
27. K.-Ch. Yu, Sh.-T. Ho, J. S. Chang, T. Jing-Song, and L.-J. Tsai, *Toxicol. Environ. Chem.*, **58**, 85 (1997).
28. D. Heil, A. Hanson, and Z. Samani, *Radioact. Waste Manage. Environ. Restoration*, **20**, 111 (1996).
29. A. Barona and F. Romero, *Water, Air, Soil Pollut.*, **95**, 59 (1997).
30. B. E. Reed, P. C. Carriere, and R. Moore, *J. Environ. Eng.*, **122**, 48 (1996).
31. J. E. van Benschoten, B. E. Reed, M. R. Matsumoto, and P. J. McGarvey, *Water Environ. Res.*, **66**, 168 (1994).
32. A. P. Davis and I. Singh, *J. Environ. Eng.*, **121**, 174 (1995).
33. H. E. Allen and P.-H. Chen, *Environ. Prog.*, **12**, 284 (1993).
34. S. B. Martin and H. E. Allen, *CHEMTECH*, **23** (April 1996).
35. R. F. Probst, R. E. Hicks, *Science*, **260**, 498 (1993).
36. L. M. Vane and G. M. Zang, *J. Hazard. Mater.*, **55**, 61 (1997), and other articles in this issue.
37. J. S. H. Wong, R. E. Hicks, and R. F. Probst, *J. Hazard. Mater.*, **55**, 61 (1997).
38. E. Juzeliunas and K. Jüttner, *Electrochim. Acta*, **43**, 1691 (1998).
39. G. Sauerbrey, *Z. Phys.*, **155**, 206 (1959).
40. R. Schumacher, *Angew. Chem.*, **102**, 347 (1990).
41. W. Stöckel and R. Schumacher, *Ber. Bunsen Ges. Phys. Chem.*, **91**, 345 (1987).
42. A. Bewick and J. Russel, *J. Electroanal. Chem.*, **132**, 329 (1982).
43. J. Benzinger, F. Pascal, S. Bernasec, M. Soriaga, and T. Hubbard, *J. Electroanal. Chem.*, **198**, 65 (1986).
44. S. Bruckenstein and M. Shay, *J. Electroanal. Chem.*, **188**, 131 (1985).
45. J. S. Gordon and D. C. Johnson, *J. Electroanal. Chem.*, **365**, 267 (1994).
46. Y. Mo, E. Hwang, and D. A. Scherson, *Anal. Chem.*, **67**, 2415 (1995).
47. J. W. Johnson, H. W. Jiang, S. B. Hanna, and W. J. James, *J. Electrochem. Soc.*, **119**, 574 (1972).
48. K. Vetter, *Elektrochemische Kinetik*, Springer Verlag, Berlin (1961).
49. K.-J. Müller, T. Bolch, and K. Mertz, *Galvanotechnik*, **79**, 172 (1988).
50. J. L. Dawson, in *The Electrochemistry of Lead*, A. T. Kuhn, Editor, p. 314, Academic Press, New York (1979).
51. M. R. Deakin and O. Melroy, *J. Electroanal. Chem.*, **239**, 321 (1988).
52. A. Ringbom, *Complexation in Analytical Chemistry*, Interscience, New York (1963).